Cell Reports, Volume *42*

Supplemental information

Vaccination provides superior *in vivo* recall capacity of SARS-CoV-2-specific memory CD8 T cells

Inga Kavazović, Christoforos Dimitropoulos, Dora Gašparini, Mari Rončević Filipović, Igor Barković, Jan Koster, Niels A. Lemmermann, Marina Babić, Đurđica Cekinović Grbeša, and Felix M. Wensveen

Supplementary Figure 1.

A)

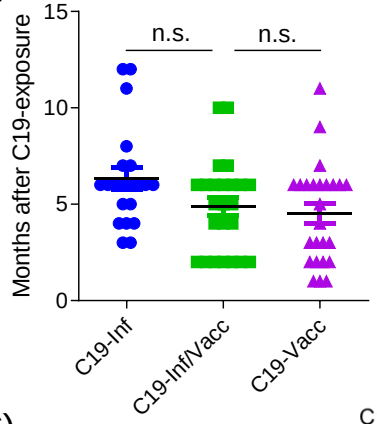

B)

	C19-Inf (21)	C19-Inf/Vacc (24)	C19-Vacc (25)
Age (yr)	55 (±15)	57 (±13)	52 (±19)
Gender (F)	9 (43%)	14 (58%)	15 (60%)
BNT162b2/BNT162b2 vaccinated	NA	21 (87.5%)	23 (92%)
mRNA-1273/mRNA-1273 vaccinated	NA	3 (12.5%)	2 (8%)
Severe disease	4 (19%)	2 (8%)	NA

C)

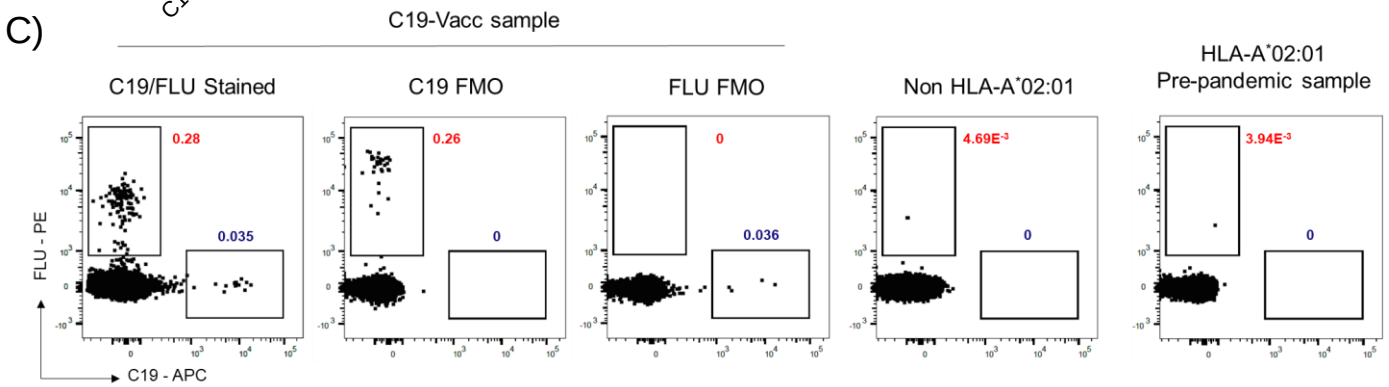

D)

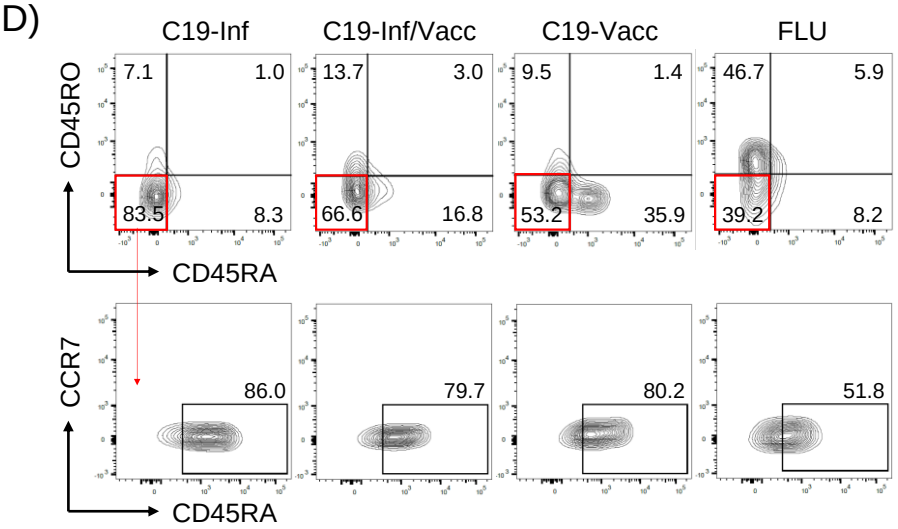

E)

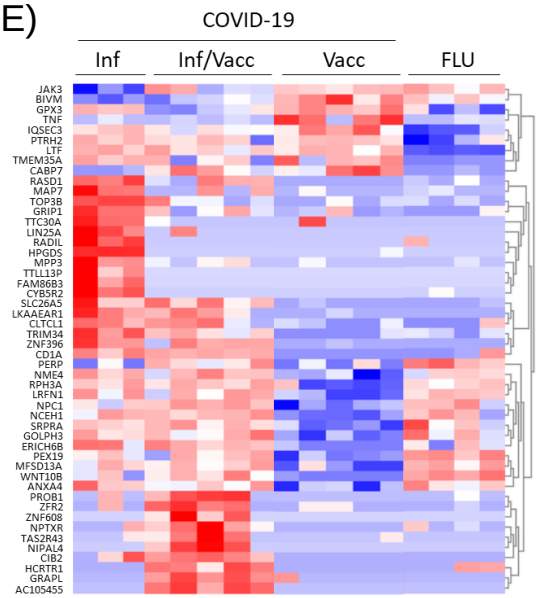

F)

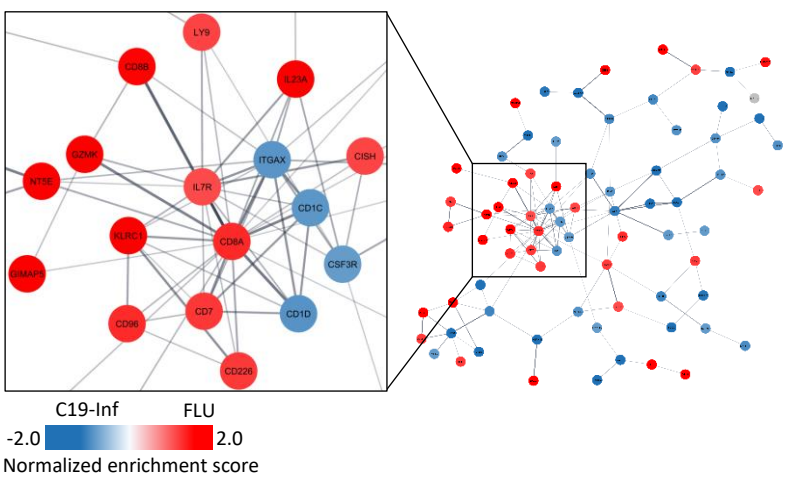

Supplementary Figure 1. Phenotypic analysis of virus-specific CD8 T cells. PBMCs from donors were analyzed directly ex vivo. (**A**) Time after last antigen exposure per group. (**B**) Study design. (**C**) Representative FACS plots of CD8+ T cell staining with HLA-A*02 tetramers: SARS-CoV-2 (YLQPRTFLL) and/or FLU (GILGFVFTL). C19-Vacc sample – non convalescent patient 1 month after 2nd dose of COVID-19 vaccine. FMO - Fluorescence Minus One (FMO) controls. Non HLA-A*02 - convalescent patient 6 months post COVID-19, negative for HLA-A*02. HLA-A*02 Pre-pandemic sample – sample from HLA-A*02^{+} individual obtained before the COVID-19 pandemic. Numbers in the plots indicate percentage of the parental population. (**D**) Representative FACS plots of CD45RO, CCR7 and CD45RA staining on C19- and FLU-specific CD8^{+} T cells of indicated groups. Quantification is shown in figure 1C. Numbers in the plots indicate percentages. (**E-F**) C19- and FLU-specific CD8^{+} T cells were sorted and analyzed by RNA sequencing. (**E**) Gene expression profile of the 50 most differentially expressed genes between the four groups. (**F**) The 200 most differentially expressed genes between C19-Inf and FLU cells were subjected to protein network clustering. Shown is the largest node network for each comparison. Inset shows the largest subcluster.

Supplementary Figure 2.

A)

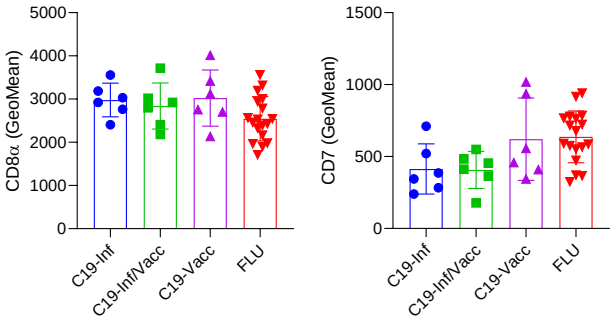

B)

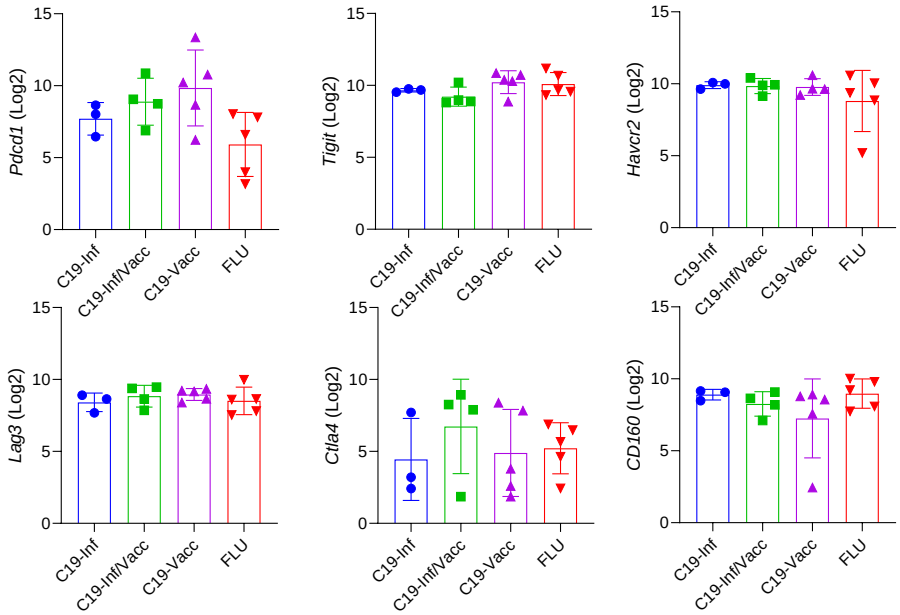

C)

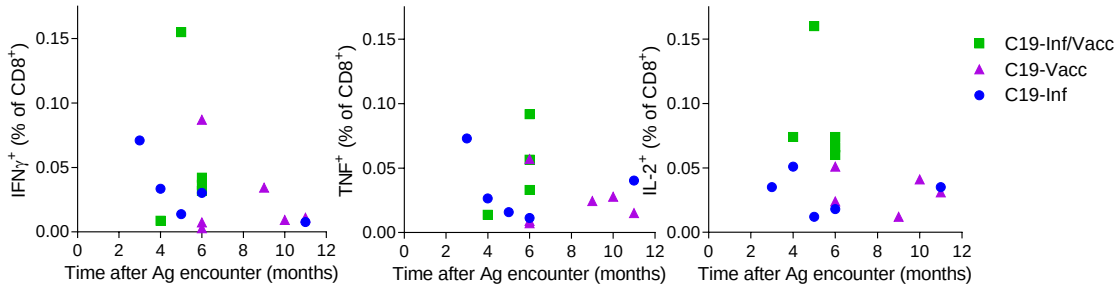

D)

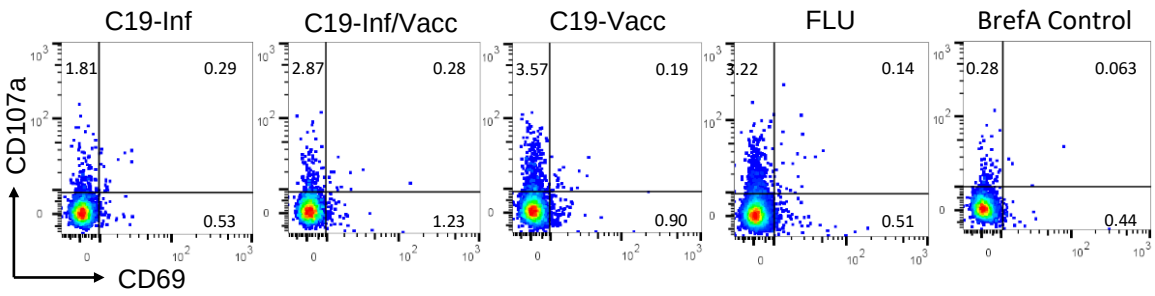

Supplementary Figure 2. Transcriptional profile of virus-specific CD8 T cells. (**A**) Geometric mean fluorescence intensity (GeoMean) of CD96, CD8, KIR2D and CD7 on C19- and FLU-specific $CD8^+$ T cells by flow cytometry. (**B**) C19- and FLU-specific CD8+ T cells were sorted and analyzed by RNA sequencing. Differential expression of individual genes associated with T-cell exhaustion are shown. Indicated are means ± s.e.m. Statistical significances at *p <0.05, **p<0.01, ***p < 0.001 by one-way ANOVA followed by Bonferroni post-testing.

Supplementary Figure 3.

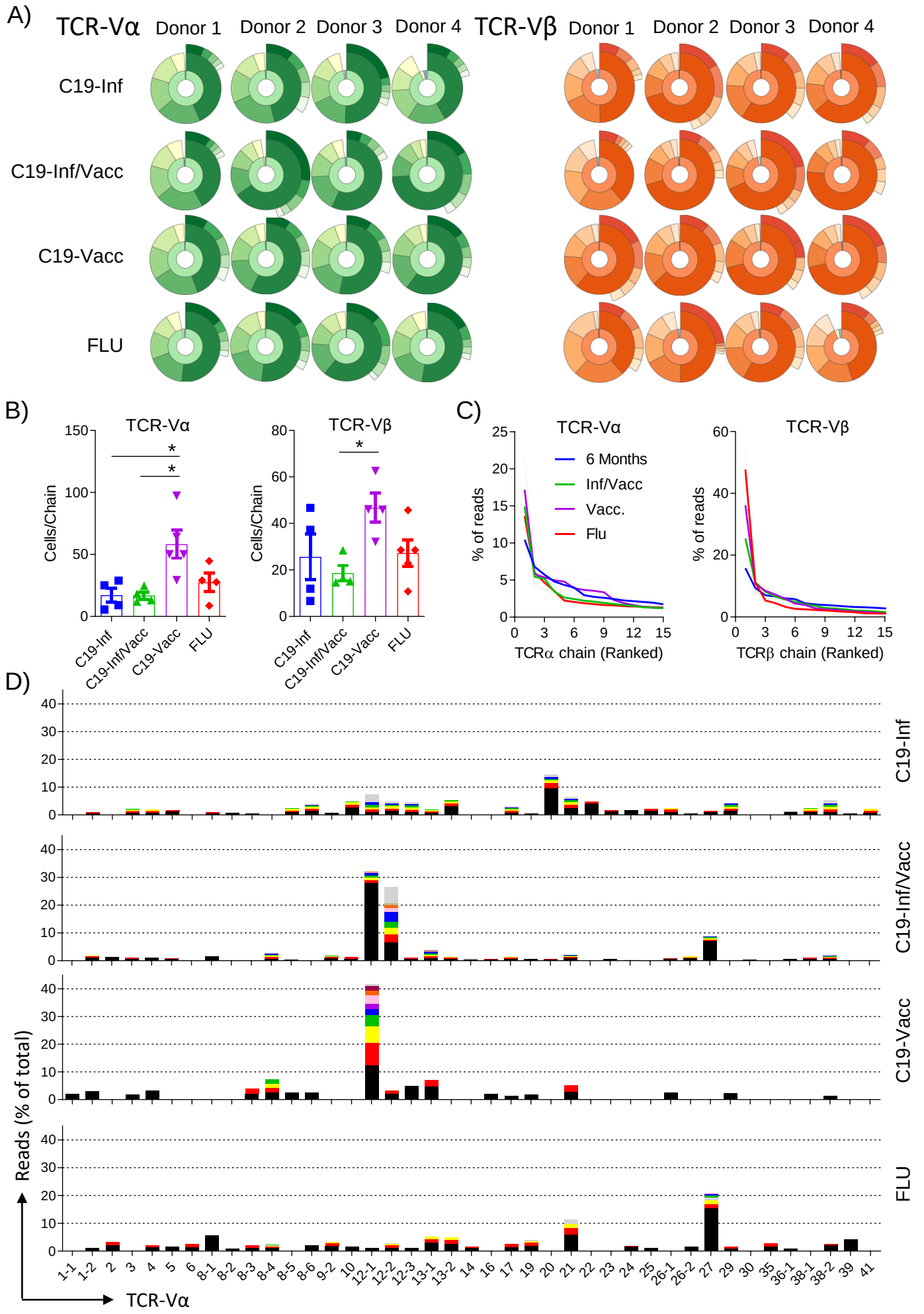

Supplementary Figure 3. Clonal analysis of virus-specific CD8 T cells. C19- and FLU-specific $CD8^+$ T cells were sorted and TCR-Vβ chains were analyzed by RNA sequencing. Contribution of the 15 most dominant TCR-Vβ genes as a percentage of the total number of clones is shown.

Supplementary Figure 4.

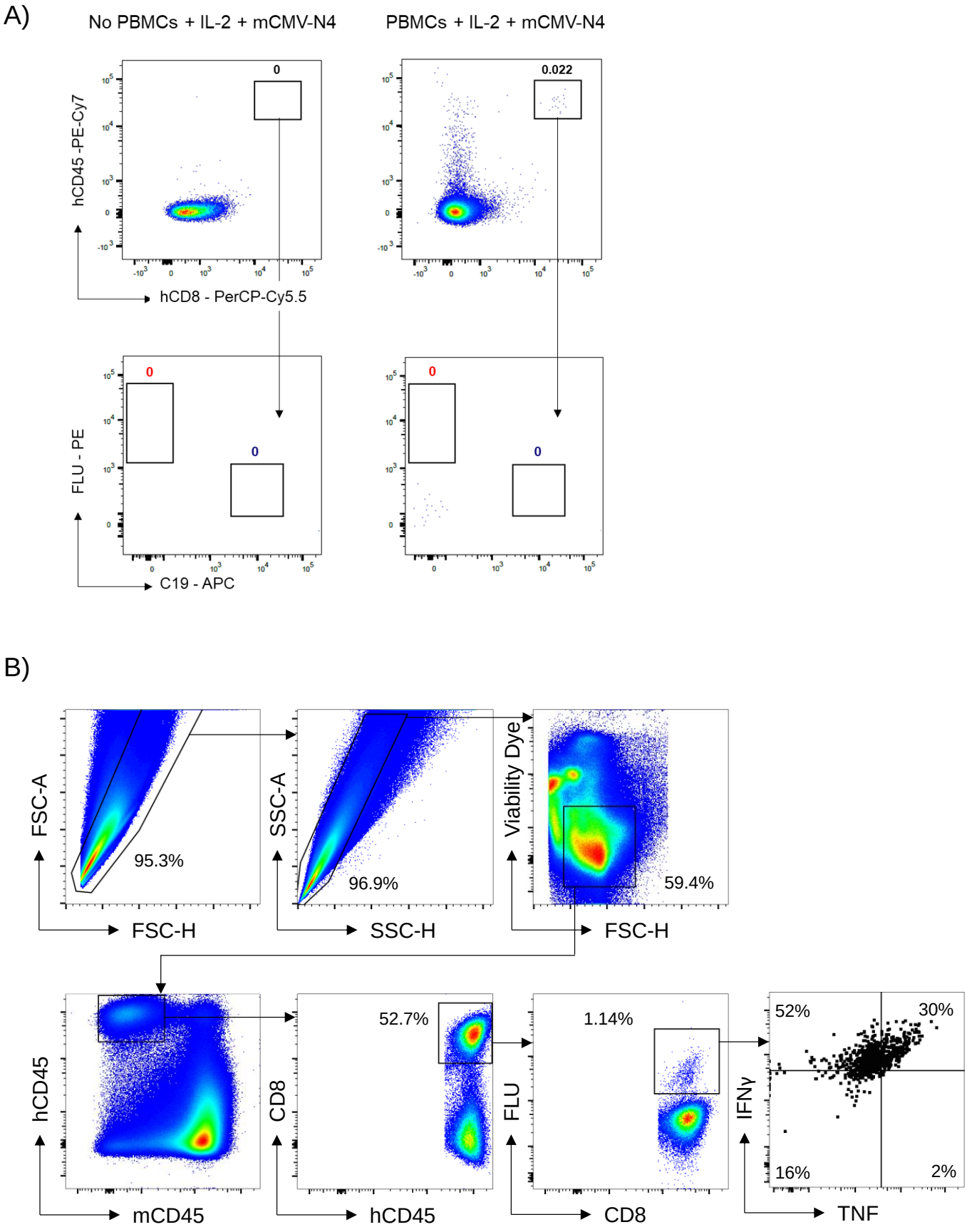

Supplementary Figure 4. Functional analysis of virus-specific CD8 T cells in vivo. Representative FACS plots of controls for Figure 5. No PBMCs (left) or PBMCs derived from a C19-vaccinated individual (right) were transferred to NSG-HLA:A*02 transgenic mice. On the same day, mice were infected i.p. with mCMV-N4. The next day mice were injected i.p. with human IL-2 (100ng/mouse). Mice were sacrificed 7 days post infection and peritoneal exudate cells (PEC) were isolated. FACS plots are showing (top) total live PEC cells and (bottom) live $hCD45^{+}hCD8^{+}$ T cells stained with HLA-A^{*}02 tetramers: SARS-CoV-2 (YLQPRTFLL) and FLU (GILGFVFTL).